Single-exhalation profiles of NO and CO_2 in humans: effect of dynamically changing flow rate

NIKOLAOS M. TSOUKIAS,[1] ZIAD TANNOUS,[2]
ARCHIE F. WILSON,[2] AND STEVEN C. GEORGE[1]
[1]*Department of Chemical and Biochemical Engineering and Materials Science and* [2]*Division of Pulmonary and Critical Care, Department of Medicine, University of California at Irvine, Irvine, California 92697-2575*

Tsoukias, Nikolaos M., Ziad Tannous, Archie F. Wilson, and Steven C. George. Single-exhalation profiles of NO and CO_2 in humans: effect of dynamically changing flow rate. *J. Appl. Physiol.* 85(2): 642–652, 1998.—Endogenous production of nitric oxide (NO) in the human lungs has many important pathophysiological roles and can be detected in the exhaled breath. An understanding of the factors that dictate the shape of the NO exhalation profile is fundamental to our understanding of normal and diseased lung function. We collected single-exhalation profiles of NO and CO_2 from normal human subjects after inhalation of ambient air (~15 parts/billion) and examined the effect of a 15-s breath hold and exhalation flow rate ($\dot{V}_E$) on the following features of the NO profile: *1*) series dead space, *2*) average concentration in phase III with respect to time and volume, *3*) normalized slope of phase III with respect to time and volume, and *4*) elimination rate at end exhalation. The dead space is ~50% smaller for NO than for CO_2 and is substantially reduced after a breath hold. The concentration of exhaled NO is inversely related to $\dot{V}_E$, but the average NO concentration with respect to time has a stronger inverse relationship than that with respect to volume. The normalized slope of phase III NO with respect to time and that with respect to volume are negative at a constant $\dot{V}_E$ but can be made to change signs if the flow rate continuously decreases during the exhalation. In addition, NO elimination at end exhalation vs. $\dot{V}_E$ produces a nonzero intercept and slope that are subject dependent and can be used to quantitate the relative contribution of the airways and the alveoli to exhaled NO. We conclude that exhaled NO has an airway and an alveolar source.

endogenous; exhalation flow rate; phase III slope; elimination rate

NITRIC OXIDE (NO) is a highly reactive and abundant molecule in the body that has many important physiological roles, including neurotransmission, host defense response, and smooth muscle relaxation (5). Recently, NO has been detected in the exhaled breath of humans (2, 21). The concentration of NO in the exhaled breath increases in inflammatory lung diseases such as bronchial asthma (15, 22). This finding generated excitement about a possible use of NO as a biomarker of pulmonary inflammation (14). In addition, exogenous NO has been shown to selectively vasodilate the pulmonary vasculature and is capable of modulating bronchial smooth muscle tone in animals and humans (8–10). The above findings suggest the possible use of NO as a therapeutic intervention for a number of pulmonary diseases. However, there is only limited information on the fundamental gas exchange dynamics of NO in the lungs.

Early studies of exhaled NO demonstrated an increase in NO elimination from the lungs with hyperventilation and exercise, providing evidence that alveolar gas contained a nonzero concentration (21). Subsequent studies demonstrated NO production from the conducting airway space below the larynx on the basis of direct measurement (24) as well as after breath hold (16, 21). The most recent studies have reported significant levels of NO in the nasal cavity (3, 16, 24). In fact, the production is approximately an order of magnitude larger in the nasal cavity than in the lower respiratory tract. These studies have documented that endogenous NO production in the airways and lungs is heterogeneous and likely plays a variety of roles in normal lung function.

The heterogeneity in the source of exhaled NO complicates the interpretation of the exhalation profile. Historically, the exhalation profile of the respiratory gases, CO_2 and O_2, and other inert gases, such as He and N_2, has provided great insight into the gas exchange dynamics of the specific gas and the lungs, in general. The shape of the NO exhalation profile has not been fully characterized. Recently, NO concentration was shown to be inversely related to exhalation flow rate ($\dot{V}_E$) (28). This result was also consistent with conducting airway production of NO and highlighted the importance of further study into the dynamics of NO gas exchange. The objective of our present study is threefold: *1*) to quantitatively characterize the features of the NO oral exhalation profile, *2*) to further explore the dependence of the NO exhalation profile on $\dot{V}_E$, and *3*) to develop an experimental technique that can provide an estimate of the relative contribution of the airways and the alveoli to exhaled NO.

METHODS

Subjects. We collected oral exhalation profiles of NO and CO_2 in seven normal men [28.4 ± 3.8 (SD) yr] with no history of smoking or lung diseases. The protocol was approved by the Institutional Review Board at the University of California, Irvine. Subjects were categorized as normal on the basis of standard spirometry that included forced vital capacity, forced expiratory volume in 1 s, and forced expiratory flow between 25 and 75% of the exhaled volume. All subjects included in the study had spirometry values >75% of predicted on the basis of their race, age, weight, and height (Table 1).

Isolation of nasal cavity. Several researchers have reported the nasal cavity as a significant source of NO in the respiratory tract (3, 16, 24) that is capable of contaminating the oral exhalation profile. Hence, to collect a true oral exhalation profile to describe the exchange dynamics of NO in the lower respiratory tract, the nasal cavity must be isolated from the lower respiratory tract. To achieve this, we applied a small negative pressure (−20 cmH_2O) to the nasal cavity. Each

Table 1. *Physical characteristics of subjects*

Subject No.	Height, cm	Weight, kg	FVC, liters	FEV_1, %pred	FEF_{25-75}, %pred
1	173	63	4.19	84	75
2	167	55	4.25	90	85
3	181	70	5.42	102	102
4	175	77	4.85	101	112
5	167	61	3.81	83	76
6	173	66	4.58	95	93
7	172	72	4.00	85	84
Mean	172.5	66.3	4.44	91.4	89.6

FVC, forced vital capacity; FEV_1, forced expiratory volume in 1 s; FEF_{25-75}, forced expiratory flow at 25–75% of exhaled volume.

subject was then instructed to swallow, which elevated the soft palate and sealed the nasal cavity. Closure of the soft palate was confirmed by monitoring the nasal cavity pressure and maintaining a nasal concentration of CO_2 of <0.5% during expiration. Any maneuvers where movement of the soft palate was detected (change in nasal cavity pressure) were discarded and repeated. All exhalation profiles had a constant negative nasal pressure between −10 and −20 cmH_2O. Under these conditions, all subjects maintained a nasal CO_2 concentration <0.5% during the course of the exhalation maneuver.

The negative nasal cavity pressure provides several advantages over other reported methods. *1*) Elevation of the soft palate requires no special effort from the subject. In contrast, balloon occlusion is invasive, and voluntary closure of the soft palate requires subject training. *2*) Minor openings of the soft palate will result in a convective flow into the nasal cavity and will not contaminate the oral exhalation. *3*) By recording the pressure in the nasal cavity, even minor openings of the soft palate can be detected immediately. *4*) The nasal cavity is isolated during inspiration and expiration.

Protocol. The design of the experimental protocol focuses on the effect of $\dot{V}_E$ on the NO exhalation profile. After isolation of the nasal cavity, each subject was asked to breathe comfortably (3–5 tidal breaths) before performing a single-exhalation maneuver. In our single exhalation a subject inspires from functional residual capacity to total lung capacity, then slowly exhales to approximately functional residual capacity. The exhalate passed through a mouthpiece connected to a "j" valve (two 1-way valves), allowing the subjects to inspire ambient air [10–15 parts/billion (ppb) NO] through one port and exhale through the second port. Gas (NO and CO_2) was measured from a sampling port at the side of the mouthpiece, ~1 cm from the mouth.

Each subject performed four different $\dot{V}_E$ patterns: *1*) constant slow $\dot{V}_E$ of ~250 ml/s (control maneuver), *2*) constant faster $\dot{V}_E$ of ~500 ml/s, *3*) linearly (in time) increasing $\dot{V}_E$, and *4*) linearly (in time) decreasing $\dot{V}_E$. Each subject performed the maneuvers in triplicate, with or without a 15-s breath hold before the exhalation. Hence, each subject performed 24 technically acceptable exhalation maneuvers (4 $\dot{V}_E$ × 3 replicates × 2 presence or absence of breath hold). Exhalation with constant flow rate was facilitated by use of a Starling resistor. The resistance to flow through a Starling resistor increases with increasing flow; thus the resistor serves to maintain a constant flow rate, independent of expiratory effort of the subject. On-line representation of the flow signal on the screen of the computer assisted the subjects during performance of the increasing and decreasing $\dot{V}_E$ maneuvers.

Airstream analysis. NO concentration was measured using a chemiluminescence NO analyzer (model NOA280, Sievers Instruments, Boulder, CO). The instrument is capable of providing highly accurate (repeatability ±1 ppb vol) gas phase measurements with a very small detection threshold [<5 ppb vol–500 parts/million (ppm) vol] and a fast response time (0–90% response time of 200 ms). We used a needle valve to restrict flow and maintain an operating reaction cell pressure of 7.5 mmHg and a sampling rate of 250 ml/min. The factory calibration values of the instrument were tested periodically using certified NO gas (27.8 ppm in N_2).

CO_2 concentration was measured by using a fast-response (0–90% response time of 100 ms) mass spectrometer (Perkin-Elmer Medical Instruments, Pomona, CA). The convective transport times for NO and CO_2 from the mouth to the analyzers were 350 and 450 ms, respectively. These times were subtracted from the profiles before analysis.

Flow rate was measured with a pneumotachometer (model 50-MC2-M2, Mariom). Analog signals from the pneumotachometer, the mass spectrometer, and the chemiluminescent analyzer were digitized through a 12-bit analog-to-digital converter. The analog-to-digital card was programmed to scan three channels simultaneously every 50 ms. The resulting measurements (20 Hz) were stored in a computer for later analysis. Figure 1 is a schematic of the experimental setup.

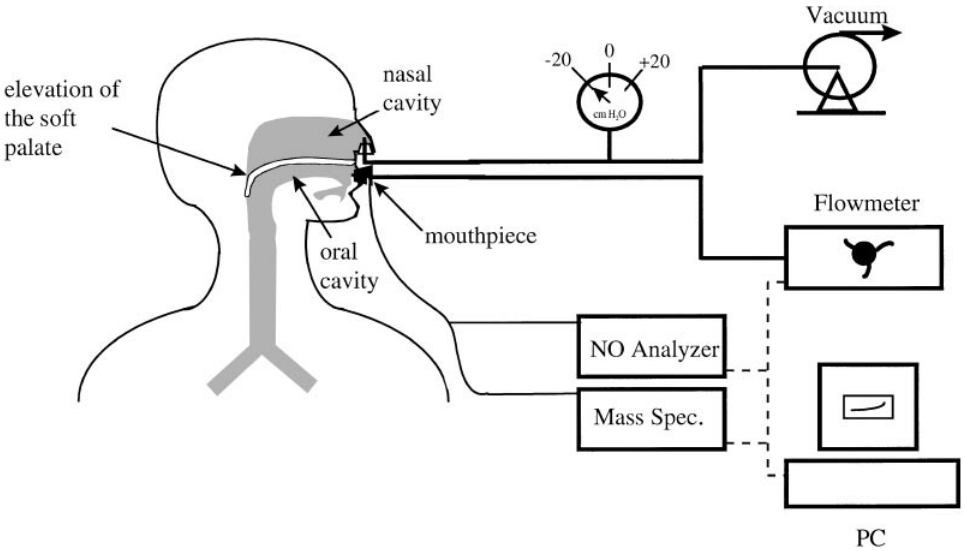

Fig. 1. Schematic of experimental setup. Soft palate was elevated with negative nasal cavity pressure (−20 cmH_2O). Exhalation flow rate was controlled with a Starling resistor in constant flow rate maneuvers. Nitric oxide (NO) concentration was measured using chemiluminescence, and CO_2 concentration was measured with mass spectroscopy. PC, personal computer.

Data analysis. We used three parameters to characterize the exhalation profile: *1*) series dead space, *2*) average concentration of phase III, and *3*) slope of phase III. In addition, we determined the elimination rate of each gas from the lungs.

The dead space for CO_2 ($V_{D_{CO_2}}$) was calculated as described by Meyer et al. (18) using backextrapolation of the phase III slope with respect to exhaled volume [$S_{III,CO_2}(V)$] (18, 19, 25, 26). Because the shape of the exhalation profile of NO is quite different from that of CO_2 (see RESULTS), we defined the dead space of NO ($V_{D_{NO}}$) in a different manner. The exhalation profile of NO is characterized by a rapid rise to an initial peak in phase I. The slope of phase III can be negative or positive depending on $\dot{V}_E$ (see RESULTS). The size of the initial peak depends on the length of breath hold. We defined $V_{D_{NO}}$ as the volume corresponding to the midpoint NO concentration between the ambient level and the initial peak value in the breath-hold maneuver.

An average value for concentration and flow rate that characterizes the exhalation profile was calculated using the data in phase III (alveolar gas) of the exhalate. Average concentrations were calculated with respect to time and exhaled volume. The average concentrations and flow rates with respect to time [$\overline{C}_{E,NO}(t)$, $\overline{C}_{E,CO_2}(t)$, and $\overline{\dot{V}}_E(t)$] were calculated over a fixed time interval of 6 s beginning 2 s after the start of exhalation and ending 8 s after the start of exhalation

$$\overline{C}(t) = \frac{\int_2^8 C\, dt}{\int_2^8 dt} \quad (1)$$

The average concentrations and flow rates with respect to volume [$\overline{C}_{E,NO}(V)$, $\overline{C}_{E,CO_2}(V)$, and $\overline{\dot{V}}_E(V)$] were calculated using the exhalate between 20% (V_{20}) and 60% (V_{60}) of each subject's vital capacity (VC)

$$\overline{C}(V) = \frac{\int_{V_{20}}^{V_{60}} C\, dV}{\int_{V_{20}}^{V_{60}} dV} \quad (2)$$

The time (2–8 s) and volume (20–60% of VC) intervals were chosen for two reasons: *1*) to provide a maximum interval common to all subjects and *2*) to guarantee that, even under the extreme conditions (maneuver with the lowest flow rate or subject with the smallest VC), the regression would exclude phase I and phase II of the exhalation profile. The technique for determining the average concentrations and flow rates is shown schematically in Fig. 2.

Phase III slopes for NO ($S_{III,NO}$), CO_2 (S_{III,CO_2}), and $\dot{V}_E$ ($S_{III,\dot{V}_E}$) were determined using linear least squares regression with respect to time and exhaled volume. The slopes with respect to time [$S_{III,NO}(t)$, $S_{III,CO_2}(t)$, and $S_{III,\dot{V}_E}(t)$] were calculated over the same time interval used in determining the average concentrations (2–8 s; Fig. 2). Phase III slopes with respect to volume [$S_{III,NO}(V)$, $S_{III,CO_2}(V)$, and $S_{III,\dot{V}_E}(V)$] were also calculated using the same volume interval used to determine the average concentrations and flow rates with respect to volume (20–60% of VC; Fig. 2). The slopes were then normalized with the appropriate average concentrations or flow rates as described above (e.g., slope with time normalized by the average value with respect to time)

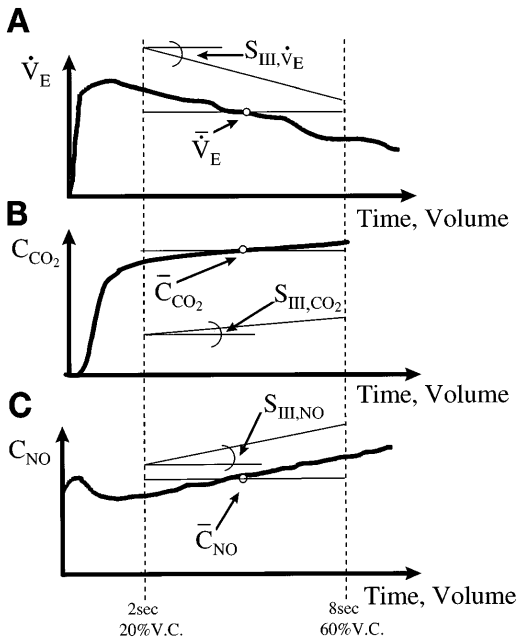

Fig. 2. Schematic detailing analysis of exhalation profiles for concentration and flow rate. Average concentrations and flow rates were estimated for exhaled volume and exhaled time by use of interval of 20–60% of vital capacity (VC) or 2–8 s, respectively. Phase III slope was calculated using linear least squares over this same interval and then normalized by average value over interval. $\dot{V}_E$, exhalation flow rate; C_{CO_2} and C_{NO}, CO_2 and NO concentration, respectively; $\overline{\dot{V}}_E$, $\overline{C}_{CO_2}$, and $\overline{C}_{NO}$, average $\dot{V}_E$, C_{CO_2}, and C_{NO}, respectively; $S_{III,\dot{V}_E}$, S_{III,CO_2}, and $S_{III,NO}$, phase III slopes for NO, CO_2, and $\dot{V}_E$, respectively.

$$\overline{S}_{III,NO}(t) = S_{III,NO}(t)/\overline{C}_{NO}(t) \quad (3)$$

$$\overline{S}_{III,CO_2}(t) = S_{III,CO_2}(t)/\overline{C}_{CO_2}(t) \quad (4)$$

$$\overline{S}_{III,\dot{V}_E}(t) = S_{III,\dot{V}_E}(t)/\overline{\dot{V}}_E(t) \quad (5)$$

$$\overline{S}_{III,NO}(V) = S_{III,NO}(V)/\overline{C}_{NO}(V) \quad (6)$$

$$\overline{S}_{III,CO_2}(V) = S_{III,CO_2}(V)/\overline{C}_{CO_2}(V) \quad (7)$$

$$\overline{S}_{III,\dot{V}_E}(V) = S_{III,\dot{V}_E}(V)/\overline{\dot{V}}_E(V) \quad (8)$$

Hence, the resulting normalized slopes represent the fractional change in gas concentration or flow rate with respect to the average per unit time or per unit volume exhaled.

The elimination rate of NO from the lungs (E_{NO}) is defined as the product of concentration and flow rate. Because concentration and flow rate are functions of time or exhaled volume, we calculated the elimination rate at end exhalation (ee). Hence, E_{NO} was determined as follows

$$E_{NO} = \dot{V}_{E,ee} C_{NO,ee} \quad (9)$$

The end-exhalation point was defined at V_{60}, and $\dot{V}_{E,ee}$ and $C_{NO,ee}$ represent average values over a period of 1 s.

E_{NO} can be simply viewed as the sum of two components: *1*) elimination from a well-mixed expansile alveolar region (product of $\dot{V}_E$ and alveolar concentration) and *2*) net airstream absorption of the gas from the tissue during transport

through the airway tree

$$E_{NO} = \dot{V}_{E,ee} C_{alv,ee} + \overline{J}_{t:g,air} A_{s,air} \quad (10)$$

where $C_{alv,ee}$ is alveolar concentration at end exhalation, $\overline{J}_{t:g,air}$ is the average (over axial position) flux ($nl \cdot s^{-1} \cdot cm^{-2}$) of NO from the airway tissue into the gas phase, and $A_{s,air}$ is the total surface area of the airways (cm^2). Recently, Silkoff et al. (28) reported a linear relationship between E_{NO} and $\dot{V}_E$ over a wide range of flow rates, which suggests that *1*) $C_{alv,ee}$ approaches a steady-state value ($C_{alv,ss}$) and *2*) $\overline{J}_{t:g,air} A_{s,air}$ is essentially constant over the examined flow rate range. The above observations were verified with the theoretical model (30). In this fashion the slope of E_{NO} vs. $\dot{V}_E$ provides an estimate of $C_{alv,ss}$, and the intercept provides an estimate of the contribution from the conducting airway space to total lung elimination.

Statistics. A two-tailed paired *t*-test was used to detect differences in the dead space between gases and between different maneuvers. The same statistical method was used to examine the effect of breath hold on the average exhaled concentrations and phase III slope. The flow rate dependence of the parameters was examined with linear least squares regression. The null hypothesis of no dependence (i.e., zero slope) was tested with a single-sample two-tailed *t*-test with use of the average slope from all seven subjects. $P < 0.05$ was considered statistically significant in all analyses.

RESULTS

Figure 3*A* represents a typical exhalation profile of NO and CO_2 under the control conditions. The $\dot{V}_E$ signal is also shown. The CO_2 profile demonstrates the well-documented dead space (phase I) followed by a rapid rise (phase II) to a sloping alveolar plateau (phase III). The exhalation profile of NO is substantially different. The initial concentration is equal to the ambient concentration (~14 ppb). Phase I is present and is visually smaller than that of CO_2 (see *Series dead space*). Phase I is characterized by an initial peak and then a slow decrease during exhalation of the alveolar gas (phase III). Hence, under the control conditions of our experiment, $S_{III,NO}$ is negative (see *Phase III slope*).

Figure 3*B* represents the exhalation profiles in the same subject after a 15-s breath hold. NO and CO_2 scales have been reduced to allow depiction of the initial NO peak. The results are typical of those presented by previous investigators. For CO_2, phase I is reduced, phase II rises to a larger concentration before the start of phase III, and phase III has a flatter slope. For NO the initial peak in phase I is much larger in magnitude (70 ppb vs. 17 ppb in this particular subject), and phase III is similar in shape.

Figure 3*C* depicts the effect of a dynamically changing flow rate on the exhalation profiles (in this case a linearly decreasing $\dot{V}_E$), again, in the same subject. The CO_2 profile does not change appreciably. However, the NO profile demonstrates marked changes. After the initial peak the concentration decreases gradually to a minimum and then begins to steadily increase. This phenomenon generates a positive phase III slope (see *Phase III slope*).

Series dead space. Mean values of $V_{D_{CO_2}}$ and $V_{D_{NO}}$ for all seven subjects, under different exhalation maneuvers, are summarized in Table 2. $V_{D_{NO}}$ is ~50–60% smaller than $V_{D_{CO_2}}$ under all conditions. $V_{D_{CO_2}}$ and $V_{D_{NO}}$ decrease significantly (~40–60%, $P < 0.05$) after a 15-s breath hold but are independent of a twofold increase in the flow rate.

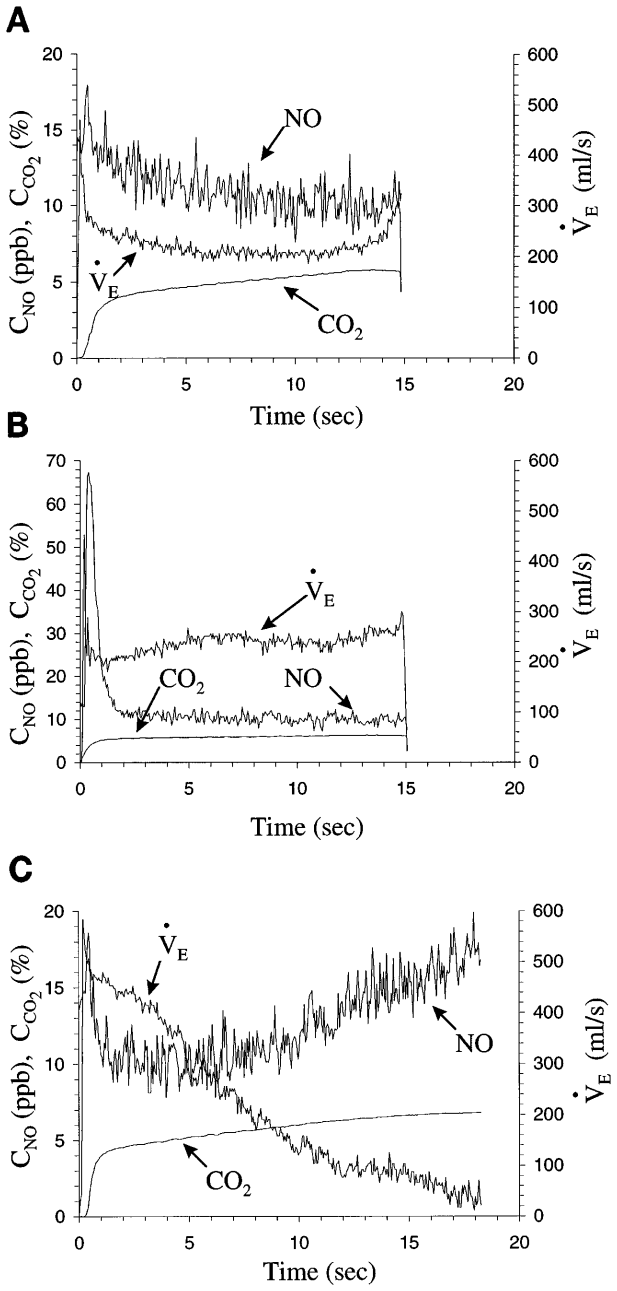

Fig. 3. Representative exhalation profiles describing qualitatively effect of $\dot{V}_E$ and breath hold. *A*: control maneuver of a constant $\dot{V}_E$ of ~250 ml/s. *B*: exhalation profiles in same subject after 15-s breath hold (note change in *y*-axis scale). *C*: exhalation profiles when $\dot{V}_E$ is decreasing linearly in time during exhalation (scale as in *A*). ppb, Parts per billion.

Average concentrations. Table 3 summarizes the average concentrations for NO and CO_2 for the control maneuver. After a 15-s breath hold, $\overline{C}_{E,NO}(t)$ and $\overline{C}_{E,NO}(V)$ were slightly decreased for most of the subjects; however, this decrease was not statistically signifi-

Table 2. *Series dead spaces*

			15-s Breath Hold	
	Slow	Fast	Slow	Fast
CO_2	180 ± 24*†	182 ± 35	77 ± 24	91 ± 14
NO	87 ± 25*	75 ± 40	34 ± 10	47 ± 11

Values are means ± SD in ml for 7 subjects. * Significantly different from breath hold ($P < 0.05$). † Significantly different from nitric oxide (NO) ($P < 0.05$).

cant. In contrast, $\overline{C}_{E,CO_2}(t)$ and $\overline{C}_{E,CO_2}(V)$ were significantly ($P < 0.05$) increased after a 15-s breath hold.

Figure 4 displays the data from the constant-flow exhalation profiles. Average concentrations for NO (Fig. 4, *A* and *B*) and CO_2 (Fig. 4, *C* and *D*) with respect to time and volume are plotted as a function of $\dot{V}_E$. The slopes for $\overline{C}_{E,NO}(t)$ and $\overline{C}_{E,NO}(V)$ were -0.0086 ± 0.0044 and -0.0048 ± 0.0039 (SD) ppb·ml^{-1}·s^{-1}, respectively. Both are statistically different from 0, indicating that $\overline{C}_{E,NO}(t)$ and $\overline{C}_{E,NO}(V)$ are inverse functions of $\dot{V}_E$. In contrast, the slopes for $\overline{C}_{E,CO_2}(t)$ and $\overline{C}_{E,CO_2}(V)$ were $+0.0006 \pm 0.0009$ and -0.0018 ± 0.0011%·ml^{-1}·s^{-1}, respectively. Only the slope for $\overline{C}_{E,CO_2}(V)$ is statistically an inverse function of $\dot{V}_E$.

Phase III slope. Relative slopes with respect to time or volume from the constant flow rate maneuvers are shown in Fig. 5. $\overline{S}_{III,NO}(t)$ and $\overline{S}_{III,NO}(V)$ did not reveal any dependence on $\dot{V}_E$. In contrast, $\overline{S}_{III,CO_2}(t)$ under control conditions is a positive function of $\dot{V}_E$, whereas under control conditions $\overline{S}_{III,CO_2}(V)$ is an inverse function of $\dot{V}_E$.

The dependence of the phase III slope on the dynamics of $\dot{V}_E$ can be illustrated by plotting $\overline{S}_{III,NO}(t)$ or $\overline{S}_{III,CO_2}(t)$ vs. $\overline{S}_{III,\dot{V}_E}(t)$. Figure 6 summarizes the data with and without breath hold for NO and CO_2. Data with significant negative or positive $\overline{S}_{III,\dot{V}_E}(t)$ were generated during the gradually decreasing or increasing flow rate maneuvers, respectively. Analysis of these slopes indicates that $\overline{S}_{III,NO}(t)$, but not $\overline{S}_{III,CO_2}(t)$, depends on $\overline{S}_{III,\dot{V}_E}(t)$ in an inverse fashion. $\overline{S}_{III,NO}(t)$ can be positive or negative depending on the slope of the flow. In contrast, $\overline{S}_{III,CO_2}(t)$ is always positive. In addition, the mean intercept on the ordinate represents the mean phase III slope at a constant flow rate [i.e., $\overline{S}_{III,\dot{V}_E}(t) = 0$]. The intercept is positive for CO_2 and negative for NO. In addition, a 15-s breath hold reduces the absolute value of the intercept for CO_2 and NO; i.e., the phase III slopes become flatter (Fig. 3*B*).

Elimination rate. E_{NO} for the constant exhalation maneuvers is displayed as a function of $\dot{V}_{E,ee}$ in Fig. 7. A 15-s breath hold had no statistical effect on the elimination rates at end exhalation; hence, all the data have been lumped together. The mean slope (an index of $C_{alv,ss}$) and intercept (an index of airway flux or production) for each subject are presented in Table 4. E_{NO} is generally a positive function of $\dot{V}_{E,ee}$; however, the standard deviation of E_{NO} is large. In fact, the slope of NO for *subject 1* was zero. The slope for all subjects, and hence the average steady-state alveolar concentration, was 5.6 ± 3.1 (SD) ppb. The intercept, and hence the average net total airway flux of NO ($\overline{J}_{t:g,air}A_{s,air}$), for the seven subjects was $0.71 \pm 0.31 \times 10^{-6}$ ml/s and is statistically different from zero.

Table 3. *Average concentrations and flow rates*

	Control	15-s Breath Hold
$\overline{C}_{E,NO}(t)$, ppb	9.35 ± 3.49	8.86 ± 3.32
$\overline{C}_{E,CO_2}(t)$, %	4.67 ± 0.23	5.68 ± 0.23*
$\dot{V}_E(t)$, ml/s	262 ± 42	255 ± 35
$\overline{C}_{E,NO}(V)$, ppb	8.98 ± 3.29	8.61 ± 3.18
$\overline{C}_{E,CO_2}(V)$, %	4.98 ± 0.26	5.83 ± 0.25*
$\dot{V}_E(V)$, ml/s	264 ± 39	264 ± 25

Values are means ± SD for 7 subjects. $\overline{C}_{E,NO}(t)$ and $\overline{C}_{E,CO_2}(t)$, average NO and CO_2 concentration with respect to time, respectively; $\overline{C}_{E,NO}(V)$ and $\overline{C}_{E,CO_2}(V)$, average NO and CO_2 concentration with respect to volume, respectively; $\dot{V}_E(t)$ and $\dot{V}_E(V)$, average exhalation flow rate with respect to time and volume, respectively; ppb, parts/billion. * Significantly different from control ($P < 0.05$).

DISCUSSION

Our experimental data suggest two different but not contradictory hypotheses: *1*) NO may originate from the airway region of the lung, which is fairly nonexpansile; *2*) NO may originate from the expansile alveolar region of the lung. The combination of *hypotheses 1* and *2* can provide a possible explanation for the unique behavior of the NO exhalation profile and the differences with CO_2 that have been observed by us and others. However, the existence of alternative explanations cannot be excluded. Some are discussed below. The relative importance or contribution of each of these mechanisms is examined in greater detail with the development of a simplified two-compartment mathematical model (30).

Series dead space. There is a significant difference between $V_{D_{CO_2}}$ and $V_{D_{NO}}$. Although $V_{D_{CO_2}}$ (180 ± 24 ml) is probably overestimated [a phenomenon previously reported (18) and attributed to an artifact arising from backextrapolation of the nonlinear CO_2 profile], $V_{D_{NO}}$ (87 ± 25 ml) is significantly smaller. Hence, even with the nasal passages isolated, NO appears in the exhaled breath before CO_2. This result is consistent with considerable production of NO in an area of the lung before the alveolar region, the source of CO_2 (*hypothesis 1*). The considerable decrease in the dead space volume for both gases after the short breath-hold time has been previously reported (4, 18) and is attributed primarily to cardiogenically induced convective mixing during the breath hold. Although the techniques used to determine $V_{D_{NO}}$ and $V_{D_{CO_2}}$ were different, they are quite similar and cannot account for the large difference between $V_{D_{NO}}$ and $V_{D_{CO_2}}$.

Average phase III concentrations. The decrease in the average exhaled concentration over the specified volume interval (20–60% of VC) in the constant flow rate maneuvers with higher $\dot{V}_E$ (Fig. 4) cannot be attributed to the same mechanism for both gases. For CO_2 this decrease can be explained through the mechanism of continuous gas exchange in the alveolar region of the lung (6, 18). Over a constant-volume interval, a slower

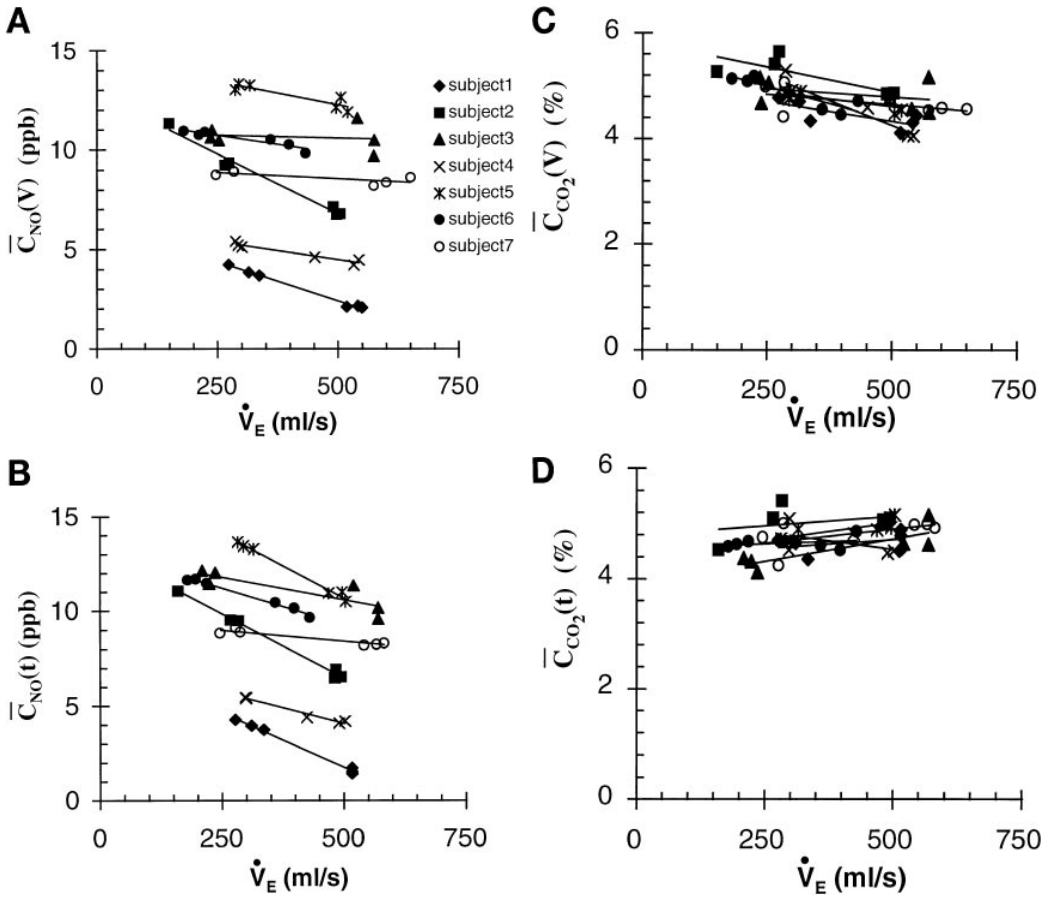

Fig. 4. $\bar{C}_{NO}$ and $\bar{C}_{CO_2}$ as a function of $\dot{V}_E$ in maneuvers where $\dot{V}_E$ was held constant throughout exhalation maneuver. *A*: $\bar{C}_{NO}$ with respect to exhalation volume [$\bar{C}_{NO}(V)$]. *B*: $\bar{C}_{NO}$ with respect to exhalation time [$\bar{C}_{NO}(t)$]. *C*: $\bar{C}_{CO_2}$ with respect to exhalation volume [$\bar{C}_{CO_2}(V)$]. *D*: $\bar{C}_{CO_2}$ with respect to exhalation time [$\bar{C}_{CO_2}(t)$]. Each subject is represented with a different symbol, and lines of linear regression are shown.

$\dot{V}_E$ will result in an increased expiration time (similar to breath holding); hence, the result is an increased CO_2 concentration due to continuous production and evolution into the alveolar gas. In contrast, when the average CO_2 concentration is calculated over a specified time interval (Fig. 4*D*), the effective time for gas exchange is the same under the different flow rate conditions. As a result, there is no statistical flow rate dependence on $\bar{C}_{CO_2}(t)$. Small changes in $\bar{C}_{CO_2}(t)$ with flow rate can be attributed to other mechanisms such as stratified or parallel inhomogeneities of the lung during exhalation (19).

In contrast, $\bar{C}_{NO}(t)$ and $\bar{C}_{NO}(V)$ are inverse functions of flow, suggesting inherently different gas exchange dynamics. The exact mechanism behind this dependence is not known. However, a probable explanation, which is in agreement with our findings for the series dead space, is that a significant part of the exhaled NO is derived from the relatively nonexpansile airway region of the lung proximal to the alveolar region (*hypothesis 1*). As $\dot{V}_E$ increases, the rate of washout in the airways (fixed volume) increases (or mean residence time decreases), thus decreasing the concentration. This phenomenon does not occur for CO_2, the source of which is the expansile alveoli. As the alveoli shrink during exhalation, CO_2 concentration in the alveolar gas is maintained relatively constant (in the absence of production or consumption) and is independent of flow rate. This concept is developed more fully in the form of a mathematical model (30). In addition, consistent with the theory of airway NO production is the fact that several cell types present in the airways, including the bronchial epithelium, fibroblast, smooth muscle cell, macrophage, and neutrophil, have been shown in vitro to produce NO and/or to contain the enzyme necessary for NO production, NO synthase (12, 13, 17, 23, 27).

Interestingly, the slope of $\bar{C}_{NO}(t)$ vs. $\dot{V}_E$ is statistically steeper than the slope of $\bar{C}_{NO}(V)$ vs. $\dot{V}_E$. If one assumes a net consumption during exhalation of NO in the alveolar region because of fast reaction with the hemoglobin of the blood in the pulmonary capillary bed, then the relationship of NO concentration to flow rate can be viewed as a result of two different antagonistic mechanisms: *1*) concentration is an inverse function of the flow due to NO production in the nonexpansile part of the lungs, and *2*) concentration is a positive function of flow as a result of a decrease in the expiration time and hence less NO consumption by the pulmonary blood. *Mechanism 2* presumes a nonzero alveolar concentration (*hypothesis 2*), which is consistent with experimentally observed in vitro production of NO by the alveolar epithelium (7) as well as theoretically by Hyde et al.

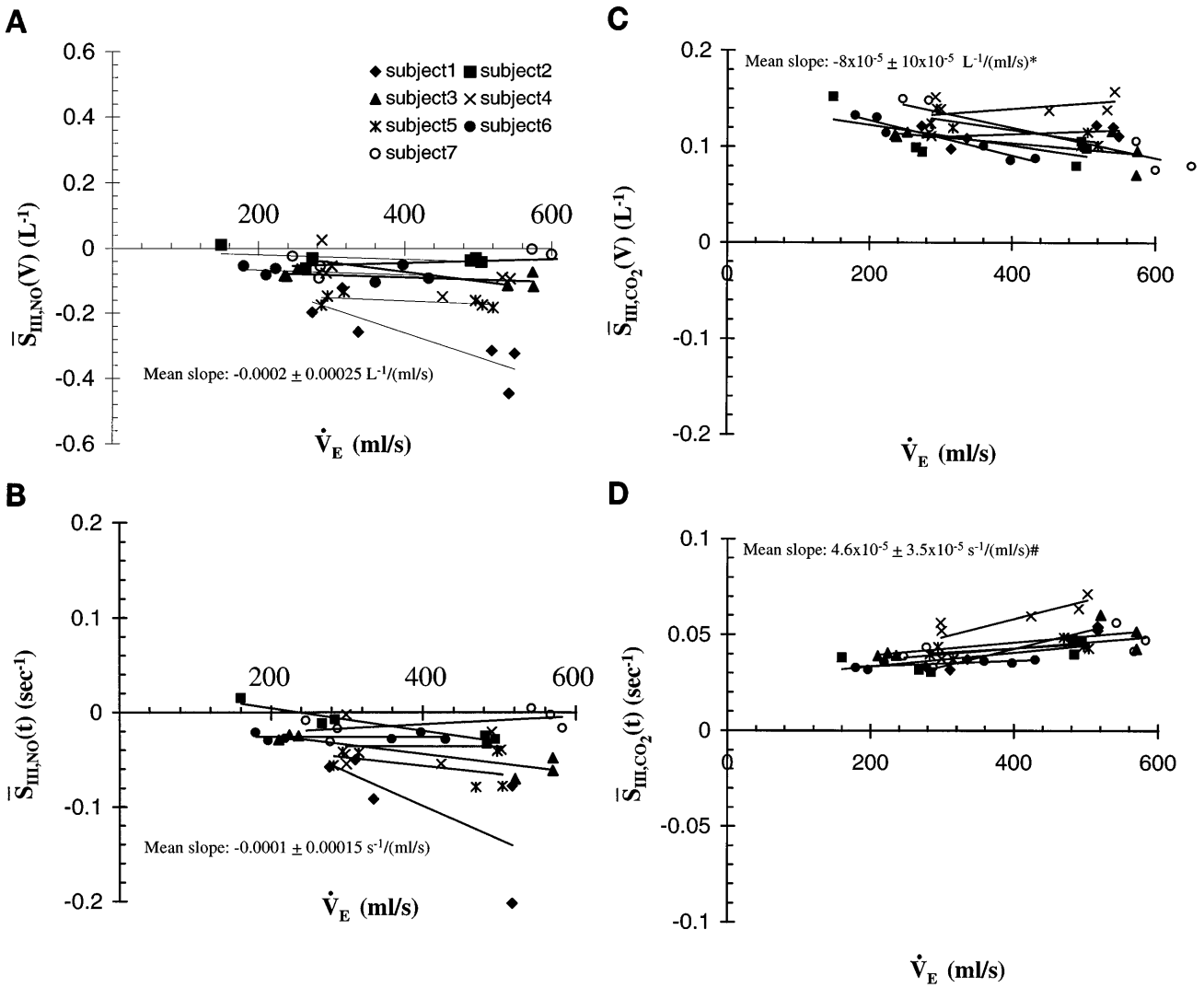

Fig. 5. Average $S_{III,NO}$ and S_{III,CO_2} ($\overline{S}_{III,NO}$ and $\overline{S}_{III,CO_2}$, respectively) as a function of $\dot{V}_E$ in maneuvers where $\dot{V}_E$ was held constant throughout exhalation maneuver. *A*: $\overline{S}_{III,NO}$ with respect to exhalation volume [$\overline{S}_{III,NO}(V)$]. *B*: $\overline{S}_{III,NO}$ with respect to exhalation time [$\overline{S}_{III,NO}(t)$]. *C*: $\overline{S}_{III,CO_2}$ with respect to exhalation volume [$\overline{S}_{III,CO_2}(V)$]. *D*: $\overline{S}_{III,CO_2}$ with respect to exhalation time [$\overline{S}_{III,CO_2}(t)$]. Statistically different from 0: $*P < 0.05$ and $\#P < 0.1$.

(11) and in our companion article (30). These two mechanisms are consistent with a steeper slope of $\overline{C}_{NO}(t)$ vs. $\dot{V}_E$ (same exhalation time and hence only *mechanism 1*) compared with $\overline{C}_{NO}(V)$ vs. $\dot{V}_E$ (different exhalation times and hence *mechanism 2* contributes).

Mechanisms other than continuing gas exchange, such as parallel or stratified inhomogeneity, may also impact the observed results. For example, parallel inhomogeneities in the lungs exist because of different alveolar ventilation-to-volume ratios. During exhalation, regions of higher ventilation will empty first from the lung and will have a lower (or higher) concentration of gas because of alveolar dilution (or enrichment) during inspiration (19). Thus, over a constant time interval, a higher $\dot{V}_E$ will increase the contribution of alveolar air in poorly ventilated regions, which have a higher (or lower) concentration. Whether the poorly ventilated regions have a higher or lower NO concentration will depend on whether there is a net positive or negative flux of NO in the specific alveolar region, respectively. A positive or negative flux depends on several factors, including the alveolar diffusing capacity, the inhaled concentration, and the volume of the specific alveolar region (11, 30). This mechanism would predict a positive or negative relationship of $\overline{C}_{NO}(t)$ to $\dot{V}_E$. Because $\overline{C}_{NO}(t)$ is a stronger inverse function of $\dot{V}_E$ than $\overline{C}_{NO}(V)$ is, parallel inhomogeneities would be an important mechanism underlying the phase III slope if a net consumption of NO occurs in poorly ventilated regions.

Recently, Silkoff et al. (28) performed an extensive study on the effect of $\dot{V}_E$ on the exhaled NO concentration during oral exhalation (nasal cavity isolated during expiration). Although they applied significant positive end-expiratory pressure, which has been reported by others to affect exhaled NO concentration (20), they also report an inverse relationship of concentration to $\dot{V}_E$.

Phase III slope. Phase III slopes have been defined in several ways by previous investigators (18, 19, 25, 26). When phase III slope data are reported, several factors

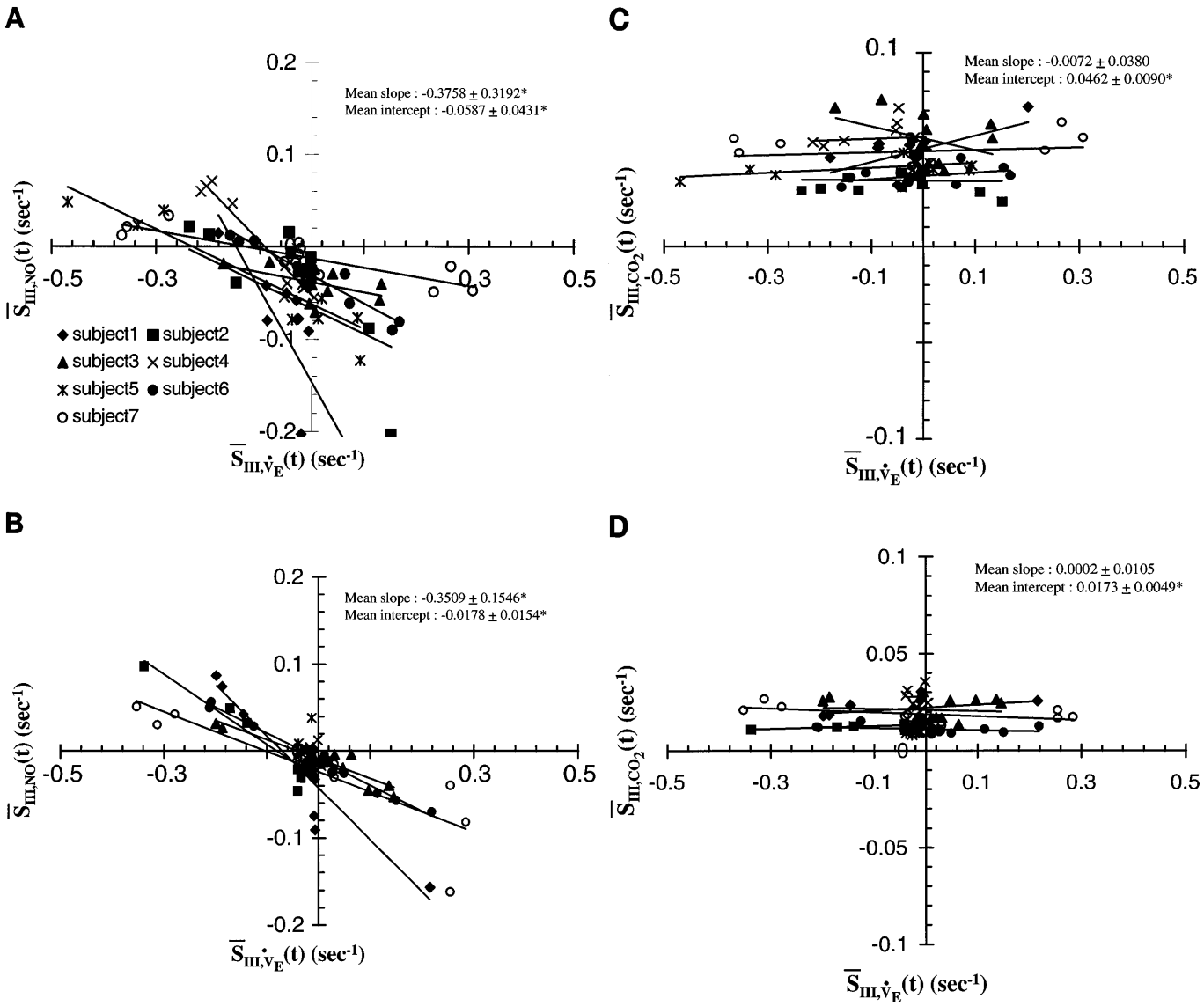

Fig. 6. $\overline{S}_{III,NO}(t)$ and $\overline{S}_{III,CO_2}(t)$ as a function of $\overline{S}_{III,\dot{V}_E}(t)$. *A*: NO without breath hold; *B*: NO with breath hold; *C*: CO_2 without breath hold; *D*: CO_2 with breath hold. Solid lines represent least squares linear regression. *Statistically different from 0 ($P < 0.05$).

must be considered: *1*) absolute vs. relative values, *2*) slope with respect to time or exhaled volume, *3*) range of the exhalation profile over which to calculate slope, and *4*) method of normalization.

We showed earlier that $\dot{V}_E$ can affect the average CO_2 concentration by changing the expiration time (continuous alveolar production) or the exhaled volume (parallel, stratified inhomogeneities). The positive dependence of $\overline{S}_{III,CO_2}(t)$ and the small negative relationship of $\overline{S}_{III,CO_2}(V)$ to $\dot{V}_E$ can be explained using the same rationale. The change in CO_2 concentration per unit time [$\overline{S}_{III,CO_2}(t)$] will increase in the constant flow rate maneuvers with a higher $\dot{V}_E$ due to parallel inhomogeneity, since the exhaled volume per unit time will increase. This change is small compared with the effect of continuing gas exchange (18). The change in CO_2 concentration per unit volume [$\overline{S}_{III,CO_2}(V)$] will slightly decrease with higher flow because of continuing alveolar gas exchange (continuous production), since the expiration time per unit volume will decrease.

If it is assumed that the average flow during the examined part of phase III does not change significantly between maneuvers, $\overline{S}_{III,CO_2}(t)$ is not expected to change with the dynamically changing flow rate maneuvers (Fig. 6, *C* and *D*). On the other hand, $S_{III,NO}$ behaves completely differently. $\overline{S}_{III,NO}(t)$ and $\overline{S}_{III,NO}(V)$ are essentially independent of the magnitude of a constant $\dot{V}_E$ but depend significantly on a changing $\dot{V}_E$ throughout the course of the single exhalation (Fig. 5, *A* and *B*, and Fig. 6, *A* and *B*).

Figure 6 displays this unique feature of the NO exhalation profile. Depending on the slope of the exhalation flow, the alveolar plateau can range from positive to negative values. The mechanisms underlying the direct relationship of the exhaled NO concentration to the flow rate presented earlier can also be invoked to

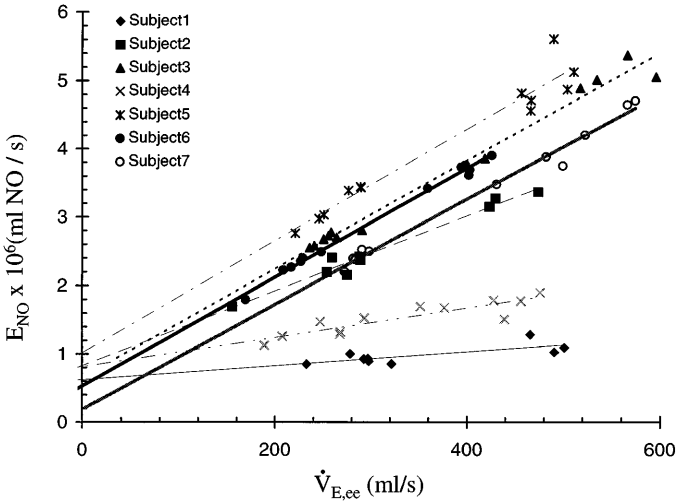

Fig. 7. Elimination rates for NO (E_{NO}) as a function of $\dot{V}_E$ at end exhalation ($\dot{V}_{E,ee}$). Only constant $\dot{V}_E$ maneuvers are shown, with and without breath hold. Lines represent least squares linear regression through all data points for each subject.

explain this phenomenon. At any given exhaled volume or time after the beginning of exhalation, an increase or decrease in $\dot{V}_E$ causes a decrease or increase in NO concentration, respectively, because of dilutional effects in the nonexpansile airways (*hypothesis 1*). For example, if $\dot{V}_E$ is continuously decreasing [i.e., negative $\overline{S}_{III,\dot{V}_E}(t)$], NO concentration will continuously increase [i.e., positive $\overline{S}_{III,NO}(t)$].

An interesting finding related to the dynamically changing flow rate maneuvers is the nonzero intercept for NO in Fig. 6, *A* and *B*. The existence of a negative $S_{III,NO}$ when $\dot{V}_E$ is constant indicates that, although the phase III slope is predominantly influenced by flow rate changes, other mechanisms also contribute. We have already suggested a nonzero alveolar concentration (*hypothesis 2*) coupled with continuing gas exchange (in the case of continuing NO consumption) as a mechanism for this negative slope. However, for continuous consumption of NO to occur in the alveolar region, alveolar concentration at end inspiration would have to be larger than the steady-state value. A steady-state alveolar NO concentration is expected when the net rate of production from the cells of the alveolar membrane is balanced by diffusion into the pulmonary blood (11, 30). Hence, it is possible that inspired conditions such as concentration and flow rate may affect the alveolar concentration at end inspiration. For example, if the inspired NO concentration were zero, then the alveolar concentration at end inspiration may be less than the steady-state value. In this case, continuing gas exchange would cause an increase in the alveolar concentration during exhalation and a positive phase III slope. This finding would be modulated by inspiration flow rate, which impacts the time of inspiration as well as absorption of NO from the airways. Our finding of a negative phase III slope may be attributed to inhaling ambient concentrations of NO that were on the order of 15 ppb. The effect of inspired conditions on the NO exhalation profile is explored further elsewhere (30) with use of a mathematical model and should be explored further experimentally.

Table 4. *Slope and intercept of E_{NO} vs. $\dot{V}_E$*

Subject No.	Slope, ppb	Intercept, ml·s^{-1}·10^6
1	1.0	0.63
2	4.3	1.12
3	7.9	0.65
4	2.2	0.81
5	8.1	1.02
6	8.1	0.59
7	7.7	0.18
Mean ± SD	5.6 ± 3.1	0.71 ± 0.31

E_{NO}, NO elimination rate; $\dot{V}_E$, exhalation flow rate.

Breath hold. The effect of breath hold on the NO and CO_2 exhalation profiles has been reported previously and can be explained in a manner consistent with the mechanisms related to average concentration and the phase III slope. During breath hold, NO and CO_2 concentrations in the airway and alveolar regions approach their steady-state values. NO accumulates in the airway space [but could also accumulate in alveoli (11)], and CO_2 accumulates in the alveolar region. Hence, during exhalation, a large initial peak in NO concentration is observed in phase I and a larger concentration of CO_2 is observed at the start of phase III.

The dynamics of NO exchange in the alveolar region are more complicated because of the somewhat unexpected result of the effect of breath hold on the average NO concentration in phase III. If continuing NO exchange in the alveolar region is the predominant mechanism underlying the negative phase III slope under control conditions (constant flow rate), then the average NO concentration in phase III should decrease after the 15-s breath hold (e.g., the alveolar concentration is expected to decrease because of consumption by the pulmonary blood). CO_2 and NO have similar relative rates of increase or decrease, respectively, during a single exhalation with constant flow rate (~5%/s over the 2- to 8-s time period without breath hold and 1.7%/s after the breath hold). However, only CO_2 concentrations were statistically affected by a breath hold. Although $\overline{C}_{E,NO}(t)$ and $\overline{C}_{E,NO}(V)$ were slightly decreased (consistent with continuous uptake by the pulmonary blood) during breath hold, this was not statistically significant. There are several possible explanations. *1*) NO consumption by the pulmonary blood may be limited and the negative $S_{III,NO}$, in contrast to S_{III,CO_2}, is generated predominantly by parallel or stratified inhomogeneities and not as a result of continuous gas exchange in the alveoli. *2*) NO concentrations in the airway space become quite elevated during the breath hold (Fig. 3*B*). The subsequent steep axial gradients in NO concentration may lead to substantial axial diffusion from NO in the airways to the alveolar region, leading to an alveolar concentration, at the end of breath hold, above its normal steady-state value. The distance of diffusion (L_D) over a 15-s breath hold can be

estimated by $L_D = 4\sqrt{D_g t}$ from an unsteady-state analysis (1). D_g is the molecular diffusivity of NO in the gas phase and is ~0.23 cm^2/s; hence, L_D is ~7.4 cm. This length spans approximately *generations 5–23* (6.5 cm) in the Weibel model (31) and easily spans the length of the respiratory bronchioles (0.62 cm in *generations 17–23*).

Elimination rate. E_{NO} did not remain constant as $\dot{V}_{E,ee}$ changed for six of the seven subjects. Although the exhaled concentration of NO decreased with increasing $\dot{V}_E$ (in the constant and in the dynamically changing maneuvers), this decrease was not sufficient to preserve a constant E_{NO} (*Eq. 9*). There are at least three explanations. *1*) As discussed earlier (*hypothesis 2*), there may be a nonzero alveolar concentration of NO. Because of the expansile nature of the alveoli, the alveolar concentration is independent of $\dot{V}_E$ (in the absence of production or consumption should alveolar concentration remain constant during exhalation). Hence, the elimination rate of a gas is proportional to $\dot{V}_E$ (*Eq. 10*). This explanation is quite probable in light of the evidence that the alveolar epithelium is capable of producing NO (7, 29). *2*) *Equation 10* suggests that a positive relationship between $\dot{V}_E$ and E_{NO} can be generated by a flow-dependent flux of NO from the airway wall ($J_{t:g,air}$). If transport of NO into the airstream within the airways is limited by diffusion in the gas phase, then increasing $\dot{V}_E$ may increase the net uptake of NO within the airways (28). As $\dot{V}_E$ increases, the concentration of NO decreases by dilution. Hence, the driving force for radial diffusion (difference between tissue concentration and airstream concentration or radial concentration gradient) is increased. The very small solubility of NO in water and tissue creates a very small relative gas-phase resistance to diffusion, making this explanation unlikely (30). The consumption of NO by chemical reaction, at least first order in NO concentration, within the airway tissue may also generate a flow-dependent flux. Increasing $\dot{V}_E$ and thus decreasing NO concentration in the airstream and within the adjacent tissue may decrease the rate of consumption by chemical reaction while the rate of endogenous production remains unaffected. It is difficult to speculate on the importance of this mechanism; however, the mathematical model provides valuable insight and suggests that reduced consumption in the airway tissue with increasing $\dot{V}_E$ is not important in explaining the observed flow rate dependence of the NO elimination.

There is a quite significant variability in the exhaled levels of NO compared with CO_2, even among normal human subjects. The large standard deviations of the intercept and slope in Fig. 6 suggest that such variability originates from the airway as well as the alveolar region of the lung. This variability can be attributed to a number of parameters, including the endogenous production of NO in the airway or alveolar tissue as well as the diffusing capacity of NO, and they are examined in detail elsewhere (30).

Conclusions. We have utilized a technique to establish satisfactory isolation of the nasal cavity while collecting the experimental oral exhalation profile of NO and CO_2 from normal human subjects. An experimental protocol was designed that focuses on the effect of $\dot{V}_E$ on the exhaled concentration of the endogenously produced gases. There are five major findings of the study related to NO exchange dynamics: *1*) the average phase III exhaled concentration of NO is an inverse function of $\dot{V}_E$; *2*) $S_{III,NO}$ is highly dependent on the dynamic changes of flow rate during exhalation and can vary from positive to negative values; *3*) for constant $\dot{V}_E$, $S_{III,NO}$ is slightly negative when ambient levels of NO are inhaled (~15 ppb); *4*) the elimination rate of NO is a positive linear function of $\dot{V}_E$ with a nonzero intercept and can be used to quantitate the relative contribution of the alveolar and airway regions to exhaled NO; and *5*) there is a large intersubject variability in exhaled NO concentration compared with CO_2. All these findings are consistent with the alveoli and the airways as sources of exhaled endogenous NO. These findings can provide directions for collecting reproducible exhalation NO profiles. For example, one must consider the following factors when assessing NO concentration in the exhaled breath: $\dot{V}_E$, exhalation volume, and region of the exhalation profile where the measurement is recorded. In addition, inspired conditions such as volume, flow rate, and concentration may impact the exhalation profile. These factors are considered by a mathematical model (30) but must also be addressed in future experimental designs.

The authors thank David S. Mukai for technical support in the collection of the exhalation profiles.

This work was supported in part by National Science Foundation Grant BES-9619340 and by generous start-up funds to S. C. George from the Department of Chemical and Biochemical Engineering and Materials Science at the University of California, Irvine.

Address for reprint requests: S. C. George, Dept. of Chemical and Biochemical Engineering and Materials Science, 916 Engineering Tower, University of California at Irvine, Irvine, CA 92697-2575.

Received 26 November 1997; accepted in final form 16 April 1998.

REFERENCES

1. **Bird, R. B., W. E. Stewart, and E. N. Lightfoot.** *Transport Phenomena*. New York: Wiley, 1960.
2. **Borland, C., Y. Cox, and T. Higenbottam.** Measurement of exhaled nitric oxide in man. *Thorax* 48: 1160–1162, 1993.
3. **Dillon, W. C., V. Hampl, P. J. Schultz, J. B. Rubins, and S. L. Archer.** Origins of breath nitric oxide in humans. *Chest* 110: 930–938, 1996.
4. **Engel, L. A., H. Menkes, L. D. H. Wood, G. Utz, J. Joubert, and P. T. Macklem.** Gas mixing during breath holding studied by intrapulmonary gas sampling. *J. Appl. Physiol.* 35: 9–17, 1973.
5. **Gaston, B., J. M. Drazen, J. Loscalzo, and J. S. Stamler.** The biology of nitrogen oxides in the airways. *Am. J. Respir. Crit. Care Med*. 149: 538–551, 1994.
6. **Gronlund, J., E. R. Swenson, J. Ohlsson, and M. P. Hlastala.** Contribution of continuing gas exchange to phase III exhaled P_{CO_2} and P_{O_2} profiles. *J. Appl. Physiol.* 62: 2467–2476, 1987.
7. **Gutierrez, H. H., B. R. Pitt, M. Schwarz, S. C. Watkins, C. Lowenstein, I. Caniggia, P. Chumley, and B. A. Freeman.** Pulmonary alveolar epithelial inducible NO synthase gene expression: regulation by inflammatory mediators. *Am. J. Physiol.* 268 (*Lung Cell. Mol. Physiol.* 12): L501–L508, 1995.
8. **Hogman, M., C. Frostell, H. Arnberg, and G. Hedenstierna.** Inhalation of nitric oxide modulates methacholine-induced bronchoconstriction in the rabbit. *Eur. Respir. J.* 6: 177–180, 1993.

9. **Hogman, M., C. G. Frostell, H. Hedenstrom, and G. Hedenstierna.** Inhalation of nitric oxide modulates adult human bronchial tone. *Am. Rev. Respir. Dis*. 148: 1474–1478, 1993.
10. **Hogman, M., S.-Z. Wei, C. Frostell, H. Arnberg, and G. Hedenstierna.** Effects of inhaled nitric oxide on methacholine-induced bronchoconstriction: a concentration response study in rabbits. *Eur. Respir. J*. 7: 698–702, 1994.
11. **Hyde, R. W., E. J. Geigel, A. J. Olszowka, J. A. Krasney, R. E. Forster, M. J. Utell, and M. W. Frampton.** Determination of production of nitric oxide by lower airways—theory. *J. Appl. Physiol*. 82: 1290–1296, 1997.
12. **Jorens, P. G., F. J. VanOverveld, H. Bult, P. A. Vermeire, and A. G. Herman.** Synergism between interleukin-1β and interferon-γ, an inducer of nitric oxide synthase, in rat lung fibroblasts. *Eur. J. Pharmacol*. 224: 7–12, 1992.
13. **Jorens, P. G., F. J. VanOverveld, H. Bult, P. A. Vermiere, and A. G. Herman.** L-Arginine-dependent production of nitrogen oxides by rat pulmonary macrophages. *Eur. J. Pharmacol*. 200: 205–209, 1991.
14. **Kharitonov, S. A., K. Alving, and P. J. Barnes.** Exhaled and nasal nitric oxide measurements: recommendations. *Eur. Respir. J*. 10: 1683–1693, 1997.
15. **Kharitonov, S. A., D. Yates, R. A. Robbins, R. Logan-Sinclair, E. A. Shinebourne, and P. J. Barnes.** Increased nitric oxide in exhaled air of asthmatic patients. *Lancet* 343: 133–135, 1994.
16. **Kimberly, B., B. Nejadnik, G. D. Giraud, and W. E. Holden.** Nasal contribution to exhaled nitric oxide at rest and during breathholding in humans. *Am. J. Respir. Crit. Care Med*. 153: 829–836, 1996.
17. **Kobzik, L., D. Bredt, C. Lowenstein, S. H. Snyder, J. M. Drazen, D. Sugarbaker, and J. S. Stamler.** Nitric oxide synthase in human and rat lung. *Am. J. Respir. Cell Mol. Biol*. 9: 371–377, 1993.
18. **Meyer, M., M. Mohr, H. Schulz, and J. Piiper.** Sloping alveolar plateaus of CO_2, O_2, and intravenously infused C_2H_2 and $CHClF_2$ in the dog. *Respir. Physiol*. 81: 137–152, 1990.
19. **Paiva, M., and L. A. Engel.** The anatomical basis for the sloping N_2 plateau. *Respir. Physiol*. 44: 325–347, 1981.
20. **Persson, M. G., P. A. Lonnqvist, and L. E. Gustafsson.** Positive end-expiratory pressure ventilation elicits increases in endogenously formed nitric oxide as detected in air exhaled by rabbits. *Anesthesiology* 82: 969–974, 1995.
21. **Persson, M. G., N. P. Wiklund, and L. E. Gustafsson.** Endogenous nitric oxide in single exhalations and the change during exercise. *Am. Rev. Respir. Dis*. 148: 1210–1214, 1993.
22. **Persson, M. G., O. Zetterstrom, V. Agrenius, E. Ihre, and L. E. Gustafsson.** Single-breath nitric oxide measurements in asthmatic patients and smokers. *Lancet* 343: 146–147, 1994.
23. **Rimele, T. J., R. J. Sturm, L. M. Adams, D. E. Henry, R. J. Heaslip, B. M. Weichman, and D. Grimes.** Interaction of neutrophils with smooth muscle: identification of a neutrophil-derived relaxing factor. *J. Pharmacol. Exp. Ther*. 245: 102–111, 1988.
24. **Schedin, U., C. Frostell, M. G. Persson, J. Jakobsson, G. Anderson, and L. E. Gustafsson.** Contribution from upper and lower airways to exhaled endogenous nitric oxide in humans. *Acta Anaesthesiol. Scand*. 39: 327–332, 1995.
25. **Scherer, P. W., S. Gobran, S. J. Aukburg, J. E. Baumgardner, R. Bartkowski, and G. R. Neufeld.** Numerical and experimental study of steady-state CO_2 and inert gas washout. *J. Appl. Physiol*. 64: 1022–1029, 1988.
26. **Schrikker, A. C. M., W. R. deVries, A. Zwart, and S. C. M. Luijendijk.** The sloping alveolar plateau of tracer gases washed out from mixed venous blood in man. *Pflügers Arch*. 413: 516–522, 1989.
27. **Shaul, P. W., A. J. North, L. C. Wu, L. B. Wells, T. S. Brannon, K. S. Lau, T. Michel, L. R. Margraf, and R. A. Star.** Endothelial nitric oxide synthase is expressed in cultured human bronchiolar epithelium. *J. Clin. Invest*. 94: 2231–2236, 1994.
28. **Silkoff, P. E., P. A. McClean, A. S. Slutsky, H. G. Furlott, E. Hoffstein, S. Wakita, K. R. Chapman, J. P. Szalai, and N. Zamel.** Marked flow dependence of exhaled nitric oxide using a new technique to exclude nasal nitric oxide. *Am. J. Respir. Crit. Care Med*. 155: 260–267, 1997.
29. **Su, W.-Y., B. J. Day, B.-H. Kang, J. D. Crapo, Y.-C. T. Huang, and L.-Y. Chang.** Lung epithelial cell-released nitric oxide protects against PMN-mediated cell injury. *Am. J. Physiol*. 271 (*Lung Cell. Mol. Physiol*. 15): L581–L586, 1996.
30. **Tsoukias, N. M., and S. C. George.** A two-compartment model of pulmonary nitric oxide exchange dynamics. *J. Appl. Physiol*. 85: 653–666, 1998.
31. **Weibel, E.** *Morphometry of the Human Lung.* New York: Springler-Verlag, 1963.